The present analysis reveals the essential plastic behavior of the sphere at sufficiently high temperatures. For an elastoplastic material, however, we can expect a thin elastic zone to exist near ρ_0. Assuming that this zone is bounded by $\rho=\rho_0(1\pm\frac{1}{2}\delta)$ where $\delta\ll 1$, and that ϵ_p at the boundaries of that elastic zone is equal to the yield strain ϵ_y, we find from Eqs. (10) by a simple expansion that $\delta\approx\rho_0\epsilon_y/\theta k$. By comparison, the result given by Cowper[1] for an elastic-perfectly plastic material reads, with the present notation, $\delta\approx 2(1-\nu)\epsilon_y/\theta k$. Both expressions for δ coincide with $n=0$ and $\nu=\frac{1}{2}$, respectively.

Finally, we mention that the present analysis is not restricted to the steady-state temperature distribution and can easily be repeated with other radial temperature gradients.

References

[1] Cowper, G. R. "The Elastoplastic Thick-Walled Sphere Subjected to a Radial Temperature Gradient," *Journal of Applied Mechanics*, Vol. 27, Sept. 1960, pp. 496-500.

[2] Johnson, W. and Mellor, P. B., "Elastic-Plastic Behaviour of Thick-Walled Spheres of Non-Work-Hardening Material Subject to a Steady State Radial Temperature Gradient," *International Journal of Mechanical Sciences*, Vol. 4, March-April 1962, pp. 147-158.

[3] Mendelson, A., *Plasticity: Theory and Application*, The MacMillan Company, New York, 1968, pp. 135-137.

AIAA 81-4147

Effect of Stiffener Eccentricity in Axially Compressed Waffle Cylinders

R. Karmakar*
Indian Institute of Technology, Kharagpur, India

Nomenclature

A_a, A_c, A_s	= axial, circumferential, and spiral stiffener area
a	= stiffener grid size
B	= extensional rigidity of plate, $Eh/(1-\nu^2)$
C_i	= stiffness parameters
D	= bending rigidity of plate, $Eh^3/12(1-\nu^2)$
d	= stiffener depth
E	= Young's modulus
h	= skin thickness
I_a, I_c, I_s	= moment of inertia of axial, circumferential, and spiral stiffener area about shell reference line
L	= cylinder length
N_{xcr}	= buckling load
$\bar{N}$	= nondimensional buckling load, N_{xcr}/ER
R	= cylinder radius
t_a, t_c, t_s	= axial, circumferential, and spiral stiffener thickness
t_{eq}	= equivalent shell thickness
$\bar{t}$	= nondimensional equivalent thickness, t_{eq}/R
α	= helix angle of spiral stiffener
$\epsilon_1, \epsilon_2, \gamma$	= reference surface strains
$\chi_x, \chi_y, \chi_{xy}$	= changes of curvature

Introduction

THE eccentricity of stiffeners has a large effect on the critical load in cylindrical shells and outside stiffening has been found to be stronger than inside stiffening.[1-4] Inversion of the stiffener eccentricity effect has been observed in cylinders under hydrostatic pressure loading.[5,6] Singer et al.[6] explained that stiffener eccentricity has two opposing effects. The primary effect is that the actual bending stiffness for outside stiffening is larger than that for inside stiffening. The secondary effect is that the actual extensional stiffness in the circumferential direction for inside stiffening is more than that for outside stiffening. This secondary effect arises out of Poisson's effect.

If the stiffener depth in a waffle cylinder is increased, the eccentricity and second moment of area of the stiffener increase. The consequent increase in actual bending stiffness causes the buckling load to increase monotonically with increase in stiffener depth.[1] The primary effect of stiffener eccentricity increases the buckling load for outside stiffening while the secondary effect decreases the same. A possible variation of the change in buckling load due to the secondary effect is shown in Fig. 1.[1] Thus, for a predominant primary effect, outside stiffening is stronger and a predominant secondary effect may cause an inversion of the stiffener eccentricity effect. This inversion is represented graphically in Fig. 2.

In this Note waffle cylinders with spiral-cum-orthogonal stiffener configuration (Fig. 3) have been analyzed for buckling under uniform axial compression. It is observed that inversion of the stiffener eccentricity effect may also occur under axial compression for this type of stiffener configuration and that the inversion is influenced by Poisson's ratio of the cylinder material.

Analysis

In an eccentrically stiffened shell-wall construction there is a coupling between extensional forces and curvature change and between bending moments and extensional strains. To account for this coupling the resultant forces and moments on a shell element may be generalized to the form

$$\begin{aligned} N_x &= C_1\epsilon_1 + C_2\epsilon_2 + C_3\chi_x + C_4\chi_y \\ N_y &= C_5\epsilon_1 + C_6\epsilon_2 + C_7\chi_x + C_8\chi_y \\ N_{xy} &= N_{yx} = C_9\gamma + C_{10}\chi_{xy} \\ M_x &= C_{11}\epsilon_1 + C_{12}\epsilon_2 + C_{13}\chi_x + C_{14}\chi_y \\ M_y &= C_{15}\epsilon_1 + C_{16}\epsilon_2 + C_{17}\chi_x + C_{18}\chi_y \\ M_{xy} &= -M_{yx} = C_{19}\gamma + C_{20}\chi_{xy} \end{aligned} \tag{1}$$

Using the method outlined in Ref. 1, the stiffness parameters are obtained as

$$C_1 = B + KA_{sa}T_1/t_{sa} \qquad C_2 = B\nu + KA_{sa}/t_{sa}$$

$$C_3 = -KA_{sa}T_1 e/t_{sa} \qquad C_4 = -KA_{sa}e/t_{sa}$$

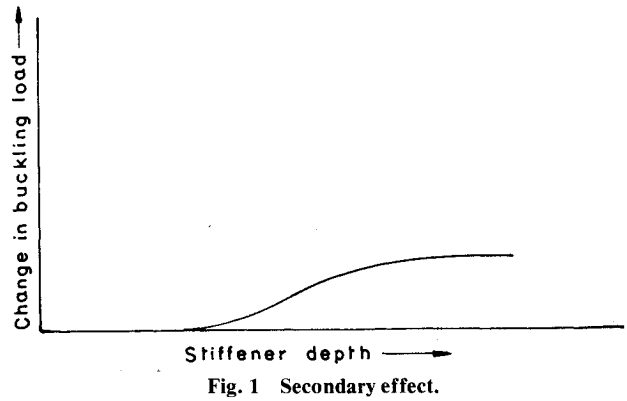

Fig. 1 Secondary effect.

Received Jan. 3, 1980; revision received Dec. 8, 1980.

*Lecturer, Department of Aeronautical Engineering.

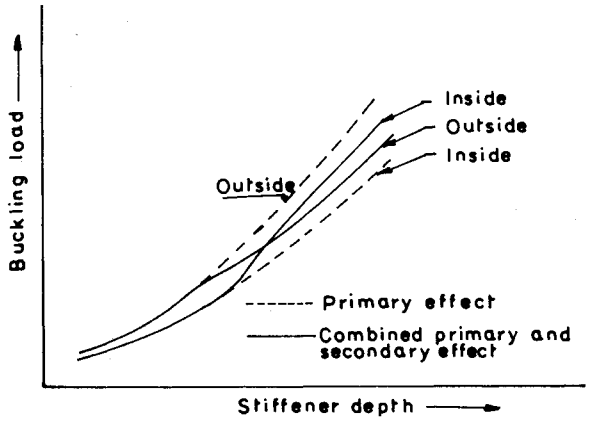

Fig. 2 Inversion of eccentricity effect.

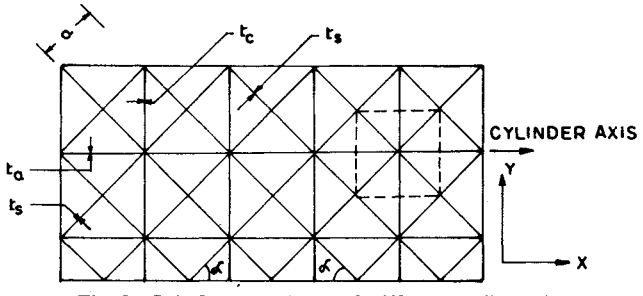

Fig. 3 Spiral-cum-orthogonal stiffener configuration.

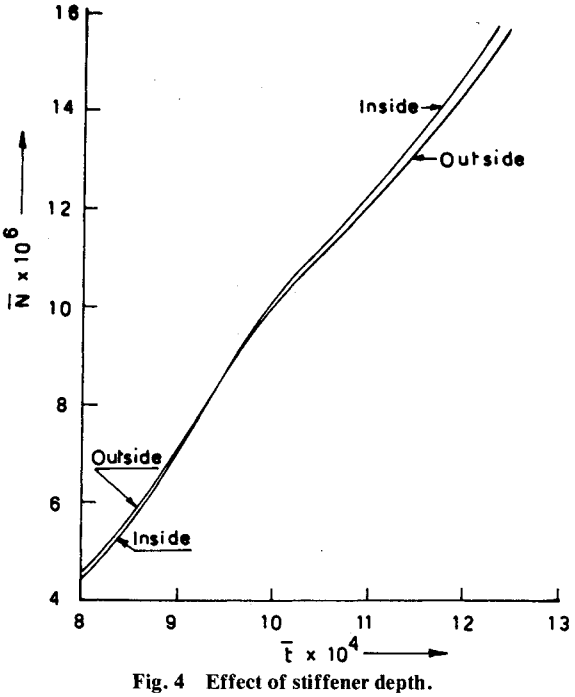

Fig. 4 Effect of stiffener depth.

$$C_5 = B\nu + KA_{sc}/t_{sc} \qquad C_6 = B + KA_{sc}T_2/t_{sc}$$

$$C_7 = -KA_{sc}e/t_{sc} \qquad C_8 = -KA_{sc}T_2e/t_{sc}$$

$$C_9 = B[(1-\nu)/2] + KA_s/t_s \qquad C_{10} = -2KA_se/t_s$$

$$C_{11} = -C_3 \qquad C_{12} = -C_4$$

$$C_{13} = -(D + KI_{sa}T_1/t_{sa}) \qquad C_{14} = -(D\nu + KI_{sa}/t_{sa})$$

$$C_{15} = -C_7 \qquad C_{16} = -C_8$$

$$C_{17} = -(D\nu + KI_{sc}/t_{sc}) \qquad C_{18} = -(D + KI_{sc}T_2/t_{sc})$$

$$C_{19} = C_{10}/2 \qquad C_{20} = D(1-\nu) + 2KI_s/t_s \qquad (2)$$

Table 1 Effect of Poisson's ratio on inversion of stiffener eccentricity effect

	$\bar{N}$ (outside)/$\bar{N}$ (inside)		
$\bar{t} \times 10^4$	$\nu = 0.3$	$\nu = 0.333$	$\nu = 0.35$
5.849	1.030	1.016	1.009
6.698	1.042	1.023	1.014
7.618	1.035	1.015	1.004
9.386	1.030	1.007	0.995[a]
11.155	1.007	0.982[a]	0.97
12.924	0.994[a]	0.968	0.955

[a] Indicates the range of $\bar{t}$ in which inversion occurs.

where

$$t_{sa} = 2t_s + t_a \qquad t_{sc} = 2t_s + t_c$$

$$A_{sa} = 2A_s + A_a \qquad A_{sc} = 2A_s + A_c$$

$$I_{sa} = 2I_s + I_a \qquad I_{sc} = 2I_s + I_c$$

$$T_1 = (t_a + 2t_s\cos^3\alpha)/2t_s\sin^2\alpha\cos\alpha$$

$$T_2 = (t_c + 2t_s\sin^3\alpha)/2t_s\sin\alpha\cos^2\alpha$$

$$K = Et_s\sin\alpha\cos\alpha/a$$

$$e = h/2 + d/2$$

For outside stiffening the sign of the stiffener eccentricity, e, is negative.

Classical buckling equations under uniform compression are expressed in terms of stiffness parameters and solved[1] for simply supported edges to obtain the critical load.

Results and Discussions

The effect of stiffener depth is studied by varying the same and plotting nondimensional buckling load $\bar{N}$ against nondimensional equivalent thickness $\bar{t}$. The results are obtained for $L = 406.4$ cm, $R = 152.4$ cm, $t_a = t_c = t_s = 0.508$ mm, $h = 0.508$ mm, $a = 101.6$ mm and $\alpha = 45$ deg. The material properties are $E = 7.326 \times 10^6$ N/cm^2 (10.6×10^6 lb/in.^{2}) and $\nu = 1/3$.

Figure 4 shows that at lower $\bar{t}$, where change in buckling load due to secondary effect is small or nonexistent, outside stiffening is slightly stronger than inside stiffening. This means the primary effect of stiffener eccentricity is small. At larger depth, change in buckling load due to secondary effect is large (Fig. 1) and causes an inversion. Thus at high $\bar{t}$, inside stiffening is stronger than outside stiffening. Since secondary effect arises out of Poisson's effect, increasing Poisson's ratio aggravates the same and, therefore, inversion should occur at smaller depth. This is verified by the results given in Table 1.

References

[1] Karmakar, R., "Buckling of Waffle Cylinders," *The Aeronautical Journal*, Vol. 83, July 1979, pp. 274-278.

[2] Van der Neut, A., "General Instability of Stiffened Cylindrical Shells under Axial Compression," National Luchtvaart Laboratorium, Amsterdam, Netherlands, Rept. S-314, 1947.

[3] Houghten, D. S. and Chan, A. S. L., "Design of a Pressurized Missile Body," *Aircraft Engineering*, Vol. 32, Nov. 1960, pp. 320-326.

[4] Baruch, M. and Singer, J., "Effect of Eccentricity of Stiffeners on the General Instability of Stiffened Cylindrical Shells under Hydrostatic Pressure," *Journal of Mechanical Engineering Science*, Vol. 5, March 1963, pp. 23-27.

[5] McElman, J. A., Mikulas, M. M., and Stein, M., "Static and Dynamic Effects of Eccentric Stiffening of Plates and Cylindrical Shells," *AIAA Journal*, Vol. 4, May 1966, pp. 887-894.

[6] Singer, J., Baruch, M. and Harari, O., "Inversion of the Eccentricity Effect in Stiffened Cylindrical Shells Buckling under Hydrostatic Pressure," *Journal of Mechanical Engineering Science*, Vol. 8, Dec. 1966, pp. 363-373.